MITSUBISHI ELECTRIC RESEARCH LABORATORIES
http://www.merl.com

Nonlinearity-tolerant Modulation Formats for Coherent Optical Communications

Kojima, K.; Koike-Akino, T.; Yoshida, T.; Millar, D.S.; Parsons, K.

TR2017-197 December 2017

Abstract

Optical fiber nonlinearity is the main factor limiting the transmission distance of coherent optical communications. We give an overview of several modulation formats which are intrinsically tolerant to fiber nonlinearity. We then describe in detail the recently proposed four-dimensional modulation format family based on 2-ary amplitude 8-ary phase-shift keying (2A8PSK), supporting spectral efficiencies of 5, 6, and 7 bits/symbol. These formats nicely fill the spectral efficiency gap between dual-polarization quadrature PSK (DP-QPSK) and DP 16-ary quadrature-amplitude modulation (DP-16QAM), with excellent linear and nonlinear performance. Since these modulation formats just use different parity bit expressions in the same constellation, similar digital signal processing can be seamlessly used for different spectral efficiency. A series of nonlinear transmission simulation results shows that this modulation format family outperforms the conventional modulation formats at the corresponding spectral efficiency. We also review DSP algorithms and the experimental results. Their application to time-domain hybrid (TDH) modulation is also reviewed.

InTech Open Book

Nonlinearity-tolerant Modulation Formats for Coherent Optical Communications

Keisuke Kojima[1], Toshiaki Koike-Akino[1], Tsuyoshi Yoshida[2,3], David S. Millar[1], Kieran Parsons[1]

[1] Mitsubishi Electric Research Laboratories (MERL), 201 Broadway Ste 8, Cambridge, MA 02139, USA, kojima@merl.com
[2] Information Technology R&D Center, Mitsubishi Electric Corporation, 5-1-1, Ofuna, Kamakura, Kanagawa 247-8501, Japan
[3] Chalmers University of Technology, SE-412 96 Gothenburg, Sweden

Abstract:

Optical fiber nonlinearity is the main factor limiting the transmission distance of coherent optical communications. We give an overview of several modulation formats which are intrinsically tolerant to fiber nonlinearity. We then describe in detail the recently proposed four-dimensional modulation format family based on 2-ary amplitude 8-ary phase-shift keying (2A8PSK), supporting spectral efficiencies of 5, 6, and 7 bits/symbol. These formats nicely fill the spectral efficiency gap between dual-polarization quadrature PSK (DP-QPSK) and DP 16-ary quadrature-amplitude modulation (DP-16QAM), with excellent linear and nonlinear performance. Since these modulation formats just use different parity bit expressions in the same constellation, similar digital signal processing can be seamlessly used for different spectral efficiency. A series of nonlinear transmission simulation results shows that this modulation format family outperforms the conventional modulation formats at the corresponding spectral efficiency. We also review DSP algorithms and the experimental results. Their application to time-domain hybrid (TDH) modulation is also reviewed.

Keywords: high-dimensional modulation format, adaptive modulation and coding, spectral efficiency, nonlinearity tolerance.

1. Introduction

Optical fiber nonlinearity is the main factor limiting the transmission distance of coherent optical communications in many cases [1]–[3]. This is an especially critical issue for low dispersion fiber case, since the waveforms stay in the original shape for a longer time and the nonlinearity effect is enhanced. In addition, in the dense wavelength multiplex division (DWDM) systems, multiple wavelength travels nearly at the same speed, so there is less opportunity of averaging out the nonlinear effects. One example is a legacy submarine cable systems [4].

At the same time, there is an increasing interest in flexible networks where adaptive transceivers select from multiple data rates, modulation formats, and forward error correction (FEC) overheads for efficient network usage [5]–[8]. For example, it has been shown that the mean loss in throughput per transceiver for a granularity of 100 Gb/s is four times larger than for a granularity of 25 Gb/s [8]. In order to cover a wide range of channel conditions, multiple modulation formats with different spectral efficiency have been extensively studied [1], [9]–[17].

In order to mitigate or minimizing the penalty from the nonlinear effects, efforts have been made to optimize the modulation formats which are intrinsically tolerant to optical fiber nonlinearity [4], [18]–[20]. In other words, the modulation format is constructed such that they are less susceptible to fiber nonlinearity. In Section 2, we discuss the so-called X-constellation, which is an eight-dimentional (8D) code and has higher nonlinearity tolerance than dual polarization (DP)-binary phase shift keying (BPSK) format of the same spectral efficiency of 2 bits/4D symbol. This significantly reduces cross polarization modulation (XPolM) and increases the transmission distance. Note that we use bits/4D symbol as a unit of spectral efficiency throughout this chapter.

Another method for reducing the fiber nonlinearity is 4D constant modulus modulation. The power of combined x- and y-polarization is constant at each time slot. This very effectively suppresses self-phase modulation (SPM) and cross-phase modulation (XPM). We discuss two earlier 4D constant modulus modulation formats [19], [20] in Section 3.

More recently proposed 4D-2A8PSK is another example of the 4D constant modulus modulation. It has been widely recognized that DP-Star-8QAM for 6 bits/symbol does not perform very well, and many formats have been investigated [21]–[25] for this spectral efficiency. In particular, 4D-2A8PSK for 6 bits/symbol has been shown to be superior to many other formats in linear and nonlinear performance, due to its large Euclidean distance, 4D constant modulus (constant power) characteristics, and Gray labeling [26]–[28]. In order to relate this to the block coding approach described in the context of high-dimensional modulation [14], 5, 6, and 7 bits/symbol modulation formats were introduced as a family of block-coded 2A8PSK in a unified manner in [29], [30].

In Section 4, we first review the modulation family 4D-2A8PSK for 5, 6, and 7 bits/symbol modulation formats. We then conduct transmission simulations in a nonlinear dispersion-managed (DM) link, as well as a dispersion-uncompensated link, to verify that this proposed modulation family indeed shows excellent linear and nonlinear transmission characteristics. Through an analysis using separated nonlinear components, we also reveal that reduction of self-phase modulation (SPM) and cross-phase modulation (XPM) are the primary beneficial factors of the 4D constant modulus property. We next discuss several items related to practical implementations in a digital signal processor (DSP), which need some attention since the constellation is different from that of the conventional QAM-based formats. Experimental verification, extension to TDH to seamlessly cover $4-8$ bits/symbol spectral efficiency, as well as the combination of combination of Grassman code and 4D-2A8PSK for the spectral efficiency of 3.5 bits/symbol.

2. X-Constellation

8-24D block codes have been proposed to achieve coding gain compared to the conventional 2D modulation formats [14], [31]–[35]. For example, using eight bit block code (four information bits and four parity bits) achieved almost 3 dB asymptotic gain. However, they are not specifically designed for nonlinearity-tolerant modulation. Shiner et al. [4] used the 8D code to achieve the coding gain, and also arranged the code such that degree of polarization (DOP) over a symbol (two time slots) becomes zero, as shown in Table I. This significantly reduces the impact of polarization change towards other channels, as well as receiving polarization effect from other channels. The authors call this modulation format "X-constellation", since the constellation of Slot-A and Slot-B are cross-polarized.

Binary Value		0000	0001	0010	0011	0100	0101	0110	0111	1000	1001	1010	1011	1100	1101	1110	1111
Slot A	x-pol	−1-i	−1-i	−1-i	−1-i	−1+i	−1+i	−1+i	−1+i	1-i	1-i	1-i	1-i	1+i	1+i	1+i	1+i
	y-pol	1+i	−1+i	1-i	−1-i	−1-i	1-i	−1+i	1+i	−1-i	1-i	−1+i	1+i	1+i	−1+i	1-i	−1-i
	$S_A = (S_1,S_2,S_3)$	(0,-4,0)	(0,0,-4)	(0,0,4)	(0,4,0)	(0,0,4)	(0,-4,0)	(0,4,0)	(0,0,-4)	(0,0,-4)	(0,4,0)	(0,-4,0)	(0,0,4)	(0,4,0)	(0,0,4)	(0,0,-4)	(0,-4,0)
Slot B	x-pol	1+i	−1+i	1-i	−1-i	1+i	−1+i	1-i	−1-i	1+i	−1+i	1-i	−1-i	1+i	−1+i	1-i	−1-i
	y-pol	1+i	−1-i	−1-i	1+i	1-i	−1+i	−1+i	1-i	−1+i	1-i	1-i	−1+i	−1-i	1+i	1+i	−1-i
	$S_B = (S_1,S_2,S_3)$	(0,4,0)	(0,0,4)	(0,0,-4)	(0,-4,0)	(0,0,-4)	(0,4,0)	(0,-4,0)	(0,0,4)	(0,0,4)	(0,-4,0)	(0,4,0)	(0,0,-4)	(0,-4,0)	(0,0,-4)	(0,0,4)	(0,4,0)
DOP	$\lvert S_A + S_B \rvert$	0	0	0	0	0	0	0	0	0	0	0	0	0	0	0	0

TABLE I
THE OPTICAL FIELD JONES VECTORS FOR THE TWO CONSECUTIVE TIME SLOTS (SLOT-A AND SLOT-B) THAT DEFINE THE 8-DIMENSIONAL X-CONSTELLATION SYMBOLS, AND THEIR CORRESPONDING BINARY SYMBOL LABELS [4].

The authors conducted a transmission experiment using 5000 km of dispersion managed high density wavelength division multiplexing (WDM) link, and compared the Q-factor of DP-BPSK and X-constellation. Fig. 1 shows that X-constellation showed 2 dB improvement in the Q-factor, demonstrating the benefit of the X-constellation.

3. 4D Constant Modulus Formats

DP-QPSK is a very robust modulation format for nonlinear transmission, and one of the main reasons is that it is 2D constant modulus, in that the power for each polarization is constant. 2D constant modulus property can also be achieved in DP-8PSK, DP-16PSK, etc., however, their Euclidean distance is smaller than that of DP-Star-8PSK and DP-16QAM, and overall transmission characteristics are not as good. Instead, 4D constant modulus modulation formats (i.e., power of the combined x- and y-polarizations is constant) were proposed. One of the 4D constant modulus format is 8PolSK-QPSK [19], in which 8 polarization states in the Stokes space representation carry 4 different absolute phases, as shown in Figs. 2. This gives 32 code words, or 5 bits/symbol spectral efficiency. Compared to DP-Star-8QAM, 8PolSK-QPSK showed significantly reduced SPM and XPM.
Another example of 4D constant modulus format is POL-QAM 6-4, where 6 polarization states carry 4 different absolute phases [20]. This gives 24 code words.

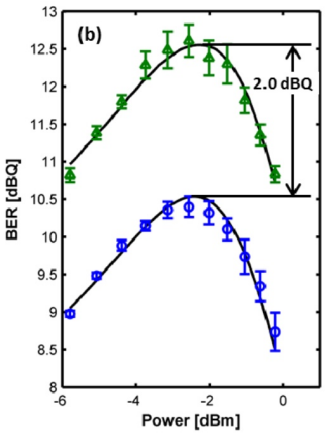

Fig. 1. The measured Q-factor for DP-BPSK (blue) and X-constellation (green) following 5000 km of high density WDM propagation [4].

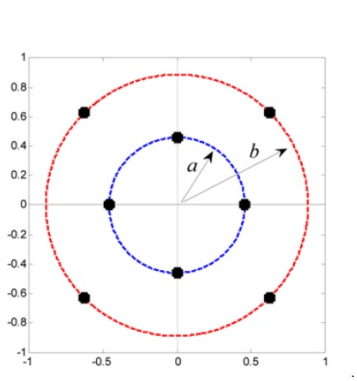

(a) Star-8QAM format. In DP-8QAM, the 2 polarizations can both independently be at amplitude a or b. For 8PolSK-QPSK format, that independence is removed.

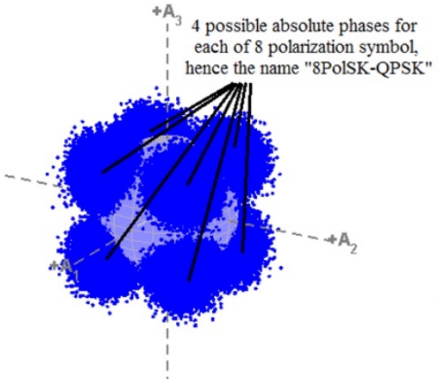

(b) Stokes space representation of the 8PolSK-QPSK with added noise giving 16 dB of SNR.

Fig. 2. 8PolSK-QPSK modulation format [19].

In the next section, we review a family of 4D-2A8PSK modulation formats, which are also 4D constant modulus formats, covering multiple spectral efficiencies, and having large coding gain.

4. 4D-2A8PSK

4.1. Generalized Mutual Information (GMI)

In order to compare the modulation formats, we first introduce a metric. Conventionally, pre-FEC bit error ratio (BER) has been used to predict post-FEC BER performance of hard decision (HD) FEC systems. However, pre-FEC BER cannot be directly applied to modern optical communications systems, which rely on soft-decision (SD) FEC coding based on bit-interleaved coded modulation (BICM). As an alternative performance measure applicable for SD-FEC systems, the BICM limit, called generalized mutual information (GMI), has been recently introduced to the optical research community for comparing multiple modulation formats [36], [37]. Several modulation formats have been compared using this metric [23], [38]. The normalized GMI can be obtained from the log-likelihood ratio (LLR) outputs of the demodulator at the receiver as follows [39]–[41]:

$$I = 1 - \mathbb{E}_{L,b}\left[\log_2\left(1+\exp\left((-1)^{b+1}L\right)\right)\right], \tag{1}$$

where b, L, and $\mathbb{E}[\cdot]$ denote the transmitted bit $b \in \{0,1\}$, the corresponding LLR value, and an expectation (i.e., ensemble average over all LLR outputs L and transmitted bits b), respectively. We denote "normalized" GMI as the mutual information per modulation bit, not per modulation symbol. The normalized GMI can thus determine the maximum possible code rate of SD-FEC coding for BICM systems. Accordingly, multiplying the number of bits per symbol with the normalized GMI is equal to the achievable throughput per symbol.
In Fig. 3, we show the relationship between Q-factor calculated from pre-FEC BER and normalized GMI of four different modulation formats, i.e., DP-QPSK, D P-Star-8QAM, 6b4D-2A8PSK, and DP-16QAM. We will explain the 6b4D-2A8PSK modulation format in detail in Section 4-4. Here, the Q-factor is defined by

$$Q^2_{\mathrm{BER}} = 2\cdot\{\mathrm{erfc}^{-1}(2\cdot\mathrm{BER})\}^2, \tag{2}$$

which is a classical measure to calculate the required signal-to-noise ratio (SNR) to achieve the BER for binary-input additive white Gaussian noise (AWGN) channels. Here, $\mathrm{erfc}^{-1}(\cdot)$ denotes an inverse complementary error function. From Fig. 3, it can be seen that the identical pre-FEC BER (Q-factor) does not achieve the same BICM limit for different modulation formats, in particular at lower code rate regimes. At the normalized GMI of 0.85, the Q-factor ranges from 4.77 dB (BER = 4.16×10^{-2}) to 4.86 dB (BER = 4.01×10^{-2}), which correspond to the typical Q (BER) threshold of the state-of-the-art SD-FEC having a code rate of 0.8 [42], [43]. Considering this fact, we will use 0.85 as a target of the normalized GMI throughout the paper.

4.2. Generic 2A8PSK

The constellation of the 4D-2A8PSK family [26]–[29] is shown in Fig. 4. It is essentially 8PSK, with two different amplitudes represented by the radii, r_1 and r_2 (suppose $r_1 \le r_2$ without loss of generality). For the combined X- and Y-polarizations (i.e., 4D space), there are $2^8 = 256$ possible combinations (i.e., 8 bits per 4D symbol). By superimposing a condition that two polarizations have complimentary radius, i.e., if r_1 is chosen for one polarization, then r_2 is used for the other

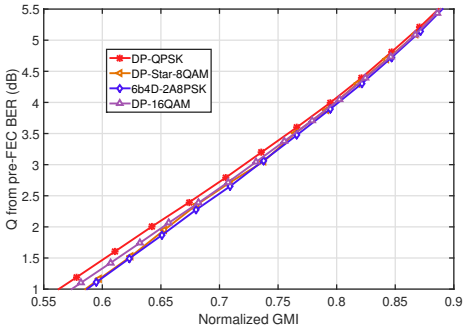

Fig. 3. Q-factor calculated from pre-FEC BER vs. normalized GMI for four modulation formats [30].

polarization, we can realize set-partitioned (SP) 4D codes, achieving 4D constant modulus property, leading to excellent nonlinear transmission characteristics. We define r_1/r_2 $(\leqslant 1)$ as a ring ratio. If the ring ratio is equal to 1, the modulation format is reduced to regular DP-8PSK. Fig. 4 also includes the mapping rule of 4D-2A8PSK [44]. Letting $B[0],\ldots,B[7]$ denote eight bits for modulation, $B[0]$–$B[2]$ and $B[3]$–$B[5]$ are used for the Gray-mapped 8PSK at X- and Y-polarizations, respectively. Whereas, $B[6]$ and $B[7]$ are used to determine the amplitude in X- and Y-polarizations, respectively. By properly choosing the best 32, 64, and 128 point constellations out of 256 combinations, we can obtain 32SP-, 64SP-, and 128SP-2A8PSK, for the spectral efficiency of 5, 6, and 7 bits/symbol, respectively. We also call these 5b4D-, 6b4D-, and 7b4D-2A8PSK for convenience.

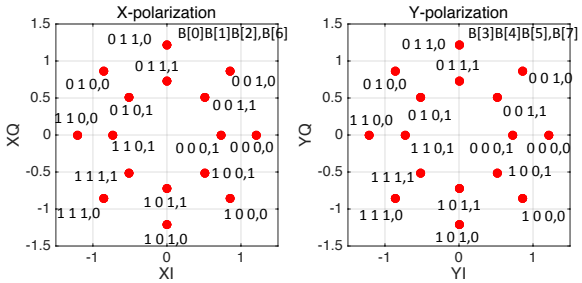

Fig. 4. Constellation and bit-to-symbol mapping of 2A8PSK [30].

4.3. 5b4D-2A8PSK

For 5 bits/symbol, 5b4D-2A8PSK (i.e., 32SP-2A8PSK) can be constructed by a linear code, with five information (modulation) bits $B[0]$–$B[4]$, and three parity bits $B[5]$–$B[7]$. Since $B[5]$ and $B[6]$

each can be expressed as the linear combination of the five information bits, the total number of possible linear codes to be designed is $2^{10} = 1024$. We selected the best combination which gives the least required SNR for the target GMI of 0.85, through Monte-Carlo simulations.
In order to realize a 4D constant modulus format, the Y-polarization ring size is always the opposite of the X-polarization ring size. This is expressed by negating another parity bit $B[6]$ for $B[7]$. Consequently, the parity-check equations for 5b4D-2A8PSK are expressed as follows:

$$B[5] = B[0] \oplus B[1] \oplus B[2], \tag{3}$$

$$B[6] = B[2] \oplus B[3] \oplus B[4], \tag{4}$$

$$B[7] = \overline{B[6]}, \tag{5}$$

where $\oplus$ and $\overline{[\cdot]}$ denote the modulo-2 addition and negation, respectively. This code shows 0.25 dB improvement in the required SNR in the linear region compared to that of [29], which was constructed as a nonlinear code.

4.4. 6b4D-2A8PSK

In the case of 6b4D-2A8PSK (64SP-2A8PSK), $B[6]$ is a parity bit of single-parity-check code which is an exclusive-or (XOR) of all the information bits $B[0]$–$B[5]$, protecting all information bits. Another parity bit $B[7]$ is the negation of $B[6]$ as used in 7b4D-2A8PSK. The best code for the target GMI of 0.85 (which we call Type A) was found to be

$$B[6] = B[0] \oplus B[1] \oplus B[2] \oplus B[3] \oplus B[4] \oplus B[5], \tag{6}$$

$$B[7] = \overline{B[6]}. \tag{7}$$

Note that this is the same code as described in [26].

4.5. 7b4D-2A8PSK

The simplest code in the 4D constant modulus 2A8PSK family is 7b4D-2A8PSK, which can also be considered as 128SP-2A8PSK. In this case, $B[0]$–$B[6]$ are the information bits while there is only one parity bit at $B[7]$. In order to realize 4D constant modulus format, a single parity bit $B[7]$ is used as follows:

$$B[7] = \overline{B[6]}. \tag{8}$$

4.6. Other Modulation Formats for Comparison

In order to evaluate the performance of 5b4D-2A8PSK, we consider three other modulation formats having 5 bits/symbol spectral efficiency; i.e., 8PolSK-QPSK [19], 32SP-16QAM [11], and time-domain hybrid (TDH) modulation. 8PolSK-QPSK [19] was described in refsec:4DConstMod. 32SP-16QAM is a 4D modulation which is based on DP-16QAM. We used the parity rule described in [11] to generate 32 code words. We also evaluated TDH modulation using a 1:1 mixture of DP-QPSK and 6b4D-2A8PSK to generate 5 bits/symbol spectral efficiency on average.

For comparison with 6b4D-2A8PSK, we evaluated three other modulation formats of 6 bits/symbol spectral efficiency; specifically, DP-8PSK, DP-Star-8QAM, and DP-Circular-8QAM [23]. DP-8PSK and DP-Star-8QAM are standard modulation formats. DP-Circular-8QAM has one center point and seven circular constellation points, and has larger Euclidean distance than DP-8PSK. We followed the constellation and labeling as described in [23].
For 7b4D-2A8PSK comparison, two more modulation formats of 7 bits/symbol spectral efficiency are evaluated. 128SP-16QAM is a 4D modulation based on DP-16QAM, where the parity rule described in [11] is used to generate 128 code words. TDH modulation using 1:1 mixture of 6b4D-2A8PSK and DP-16QAM is also simulated. In addition, we simulated $(7/8) \times 34$GBd DP-16QAM to compare for the same data rate.

4.7. Nonlinear Transmission Characteristics

1) Simulation Procedure:
We simulated transmission performance over a 2,000 km DM link at a rate of 34 GBaud per channel to investigate the effect of high fiber nonlinearity. At the transmitter, pulses were filtered by a root-raised-cosine (RRC) filter with a roll-off factor of 10%. Eleven WDM channels using the same modulation format were simulated with 37.5 GHz spacing and no optical filtering. The link comprised 25 spans of 80 km non-zero dispersion shifted fiber (NZDSF) with loss compensated by Erbium-doped fiber amplifiers (EDFAs). In order to quantify performance over the nonlinear fiber link for multiple modulation formats, a span loss budget was used as a performance metric [46], which is defined as,

$$\begin{aligned}\text{Span Loss Budget} = 58 + P - \text{ROSNR} \\ - 10\log_{10}(N) - \text{NF},\end{aligned} \tag{9}$$

where P is the launch power per channel expressed in dBm, ROSNR is the required OSNR to achieve the target GMI in dB, N is the number of spans, and NF is the noise figure of the EDFAs in dB.
NZDSF parameters were, $\gamma = 1.6$ /W/km; $D = 3.9$ ps/nm/km; $\alpha = 0.2$ dB/km. Other fiber effects such as dispersion slope and polarization mode dispersion (PMD) were not simulated. At the end of each span, 90% of the chromatic dispersion was compensated as a lumped linear dispersion compensator. Dispersion pre-compensation was applied at the transmitter side using 50% of the residual dispersion of the full link. The rest of the dispersion is compensated just before the receiver.
An ideal homodyne coherent receiver was used, with an RRC filter with a roll-off factor of 10%, followed by sampling at twice the symbol rate. For adaptive equalization, we used a time-domain data-aided least-mean-square equalizer which uses the transmitted data directly as the training sequences for simplicity. A discussion on a more realistic equalizer will be given in Section 4-9. We did not use carrier phase estimation (CPE) in Sections 4-7 and 4-8.
All the optical noise due to the EDFA is loaded just before the receiver. In order to evaluate the system margin, we varied the optical signal-to-noise ratio (OSNR) with excessive noise loading such that the target GMI is reached. The obtained required OSNR is used to calculate the span loss budget as in (9). An EDFA noise figure of 5 dB is assumed for the span loss budget calculations.
Note that in DM links it is known that there is some difference in simulated nonlinear transmission performance between having all noise loaded at the receiver (our case) and distributed noise

at each EDFA, depending on the modulation format [47]. For XPolM and WDM (SPM+XPM+XPolM) cases the difference is generally small, whilst for SPM and XPM the noise-loaded case may somewhat underestimate the nonlinear impact (where the performance gap is smaller at baud rates ≥ 28 GBaud). More detailed analysis regarding this gap is beyond the scope of this work.

2) 5 bits/symbol Formats:
Four 5 bit/symbol formats were compared as shown in Fig. 5. In this case, the ring ratio $r_1/r_2 = 0.61$ is optimized for 5b4D-2A8PSK for maximizing the span loss budget. Note that ring ratio is not a sensitive parameter, and in fact between 0.56 and 0.66, the peak span loss budget changed only by 0.03 dB.
The span loss budget for 32SP-16QAM reduces quickly due to large power variations, since it is based on 16QAM. On the other hand, 8PolSK-QPSK [19] has 0.65 dB worse OSNR for the linear case, the saturation characteristics is very similar to 5b4D-2A8PSK, due to its 4D constant modulus property. TDH modulation using a 1:1 mixture of DP-QPSK and 6b4D-2A8PSK has constant modulus property at each time slot. However, we used an optimized power allocation for TDH modulation (i.e., 6b4D-2A8PSK has 2.7 dB higher power than DP-QPSK), and there is a power fluctuation between time slots, causing some penalty due to the nonlinearity.
Overall, 5b4D-2A8PSK has the higher maximum span loss budget by 0.5 dB over the TDH modulation, by 0.9 dB over 8PolSK-QPSK, and by 1.8 dB over 32SP-16QAM.

3) 6 bits/symbol Formats:
Four 6 bits/symbol modulation formats were compared as in Fig. 6. The optimized ring ratio was $r_1/r_2 = 0.65$ for 6b4D-2A8PSK to maximize the span loss budget. It is observed that the maximum span loss budget for 6b4D-2A8PSK is higher than DP-Circular-8QAM, DP-8PSK, and DP-Star-8QAM by 0.6 dB, 0.5 dB, and 1.6 dB, respectively.

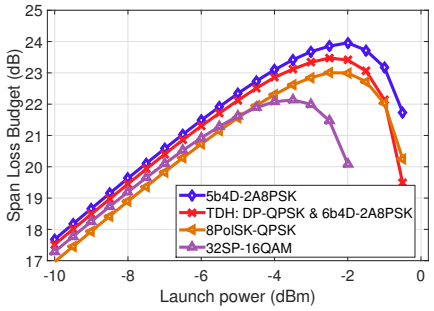

Fig. 5. Span loss budget of four 5 bits/symbol modulation formats as a function of launch power for the DM link [30].

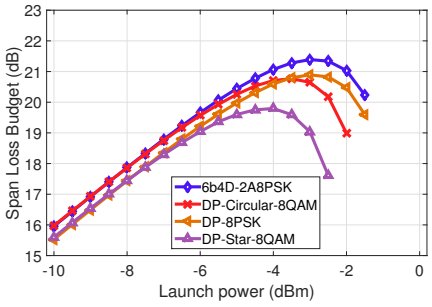

Fig. 6. Span loss budget of four 6 bits/symbol modulation formats for the DM link [30].

4) 7 bits/symbol Formats:
Fig. 7 shows performance comparison among three 7 bit/symbol formats at 34 GBd and DP-16QAM of the same data rate ($7/8 \times 34$ GBd). Here, the ring ratio of $r_1/r_2 = 0.59$ is chosen for 7b4D-2A8PSK to maximize the span loss budget. Here, TDH modulation uses a 1:1 mixture of 6b4D-2A8PSK and 128SP-QAM, whose optimized power ratio was 0.1 dB. We can see that

7b4D-2A8PSK outperformed THD modulation, 128SP-16QAM, and $(7/8) \times 34$GBd DP-16QAM by 0.7 dB, 1.4 dB, and 2.2 dB, respectively.

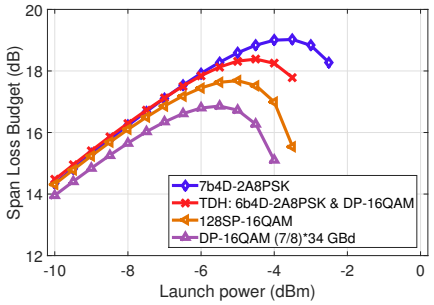

Fig. 7. Span loss budget of three 7 bits/symbol modulation formats at 34 GBd and DP-16QAM with the same data rate ($7/8 \times 34$ GBd) as a function of launch power for the DM link [30].

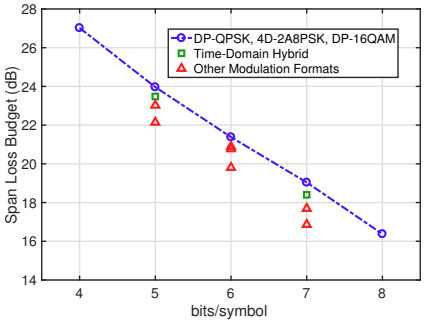

Fig. 8. Summary of the peak span loss budget for the DM link. Blue circles connected with lines are for the three 4D-2A8PSK formats, DP-QPSK, and DP-16QAM. Green squares are for TDH modulation formats, and red triangles are for other modulation formats shown in Figs. 5–7 [30].

5) Summary for DM Link:
The summary of the peak span loss budget for the DM link is shown in Fig. 8. The circles connected by the dashed lines include DP-QPSK, 5b4D-, 6b4D-, 7b4D-2A8PSK, and DP-16QAM, all at 34 GBd. Squares are taken from TDH modulation formats, and triangles are from other modulation formats in Figs. 5–7. This shows that the 4D-2A8PSK family fills the gap between DP-QPSK and DP-16QAM almost linearly (in the dB domain), and each one offers a solid improvement compared to the conventional modulation formats. Also, note that DP-QPSK is a member of 4D-2A8PSK family with specific parity-check equations and ring ratio of 1.

6) 5 bits/symbol in Dispersion Uncompensated Link: In order to evaluate the transmission characteristics of various modulation formats under a reduced nonlinearity situation, we also simulated the link with 50 spans of 80 km standard single mode fiber (SSMF) without inline dispersion compensation. SSMF parameters are, $\gamma = 1.2$ /W/km; $D = 17$ ps/nm/km; $\alpha = 0.2$ dB/km. No dispersion pre-compensation was used. The target GMI remained the same at 0.85. Fig. 9 shows the span loss budget of the four modulation formats for the spectral efficiency of 5 bits/symbol, as an example. Overall, the differences among the modulation formats are smaller than the case of DM-NZDSF link. 5b4D-2A8PSK still shows the highest budget, outperforming TDH of DP-QPSK and 6b4D-2A8PSK, 8PolSK, and 32SP-8QAM by 0.2 dB, 1.0 dB, and 0.8 dB, respectively. For dispersion uncompensated links, TDH and 32SP-16QAM did not suffer as much as they did in the DM case. This may be due to the weaker nonlinear distortion in the uncompensated SSMF links compared to DM-NZDSF links.

4.8. Separated Nonlinear Effects

In order to understand the source of the benefit of 4D constant modulus modulation, we conducted additional simulations with separated nonlinear components, based on the method pro-

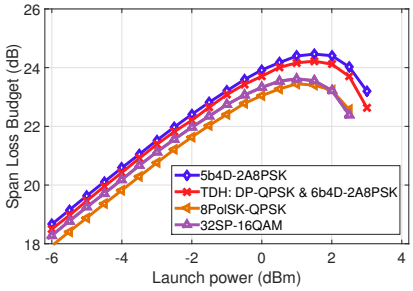

Fig. 9. Span loss budget of four 5 bits/symbol modulation formats as a function of launch power for the dispersion unmanaged link [30].

posed in [48]. Using this method, we can evaluate the nonlinear transmission performance with selective nonlinear effects of SPM, XPM, and XPolM.

In Fig. 10, we plot the calculated Q-factor as a function of the OSNR for 6b4D-2A8PSK and DP-Star-8QAM in the DM link (same simulation parameters as Section 4-71). Here, we use the recently proposed Q-factor definition based on GMI not pre-FEC BER, as follows [44]:

$$Q^2_{\mathrm{GMI}} = \{0.5 \cdot J^{-1}(\mathrm{GMI})\}^2, \tag{10}$$

where $J^{-1}(\cdot)$ is the inverse J function, widely used in extrinsic information transfer chart analysis [39]. The inverse J function is well approximated by

$$J^{-1}(I) \simeq \begin{cases} a_1 I^2 + b_1 I + c_1\sqrt{I}, & 0 \le I \le I^*, \\ -a_2 \ln[b_2(1-I)] - c_2 I, & I^* \le I \le 1, \end{cases} \tag{11}$$

$$\begin{aligned} &I^* = 0.3646, \\ &a_1 = 1.09542, \quad b_1 = 0.214217, \quad c_1 = 2.33727, \\ &a_2 = 0.706692, \quad b_2 = 0.386013, \quad c_2 = -1.75017. \end{aligned}$$

The above Q-factor based on GMI in (10) is a generalized extension from the conventional Q-factor based on BER in (2) so that we can measure the effective SNR to achieve same post-FEC BER performance with SD-FEC systems. While both definitions provide exactly same Q performance in binary-input AWGN channels, the generalized Q-factor can predict SNR gain more accurately compared to the conventional Q-factor for BICM systems using high-order high-dimensional modulation and SD-FEC coding.

The curves denoted with 'AWGN' in Fig. 10 show the case when the nonlinear effects are ignored, and the curves represented with 'SPM', 'XPM', and 'XPolM' indicate that these nonlinear components are added individually. The curve with 'SPM+XPM+XPolM' shows the case when all of these nonlinear effects are taken into account. The launch power is set to be -4 dBm, which gives the maximum span loss budget for DP-Star-8QAM. OSNR of 15.2 dB corresponds to a normalized GMI of 0.85 at this launch power.

Fig. 11 re-plots the simulated Q versus separated nonlinearity under the condition of 15.2 dB OSNR. Q in the linear case (AWGN) is higher for 6b4D-2A8PSK than DP-Star-8QAM by 0.4 dB. The contributions from SPM and XPM in 6b4D-2A8PSK are much smaller than those in DP-Star-8QAM. It verifies that 4D-2A8PSK family can be robust against XPM and SPM nonlin-

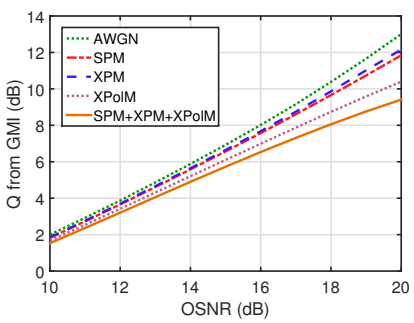

(a) 6b4D-2A8PSK

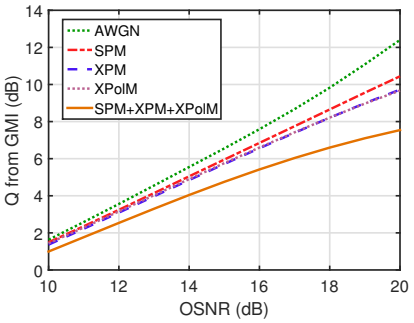

(b) DP-Star-8QAM (Curves for XPM and XPolM overlapping)

Fig. 10. Q-factor as a function of OSNR for 6b4D-2A8PSK and DP-Star-8QAM with separated nonlinear effects at a launch power of −4 dBm [30].

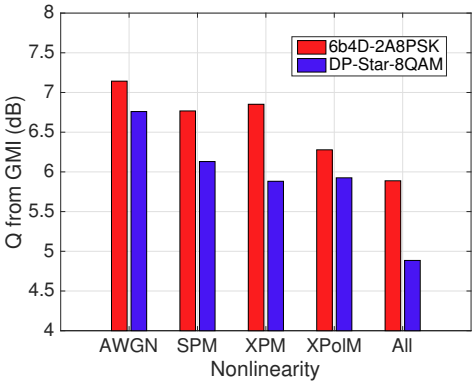

Fig. 11. Q-factor for 6b4D-2A8PSK and DP-Star-8QAM with separated nonlinear effects at a launch power of −4 dBm and OSNR of 15.2 dBm [30].

earity. On the other hand, the contribution of XPolM is similar in 6b4D-2A8PSK and DP-Star-8QAM (more specifically, Q degradation from AWGN is comparable for both modulation formats). This is because power in the individual polarization in 6b4D-2A8PSK fluctuates over symbol time even though this has a 4D constant modulus property. This result is consistent with the report in [19], where another 4D constant modulus modulation format 8PolSK shows a significant reduction in SPM and XPM, but not XPolM.

As explained in Section 4-71, we assumed PMD to be zero. In reality, PMD varies from fiber plant to fiber plant, and XPolM is generally decreased by higher PMD [49]. As shown in Figs. 10–11, the dominant nonlinear degradation for 4D-2A8PSK comes from XPolM, and hence, the benefit of 4D-2A8PSK family may be even more significant in the presence of high PMD.

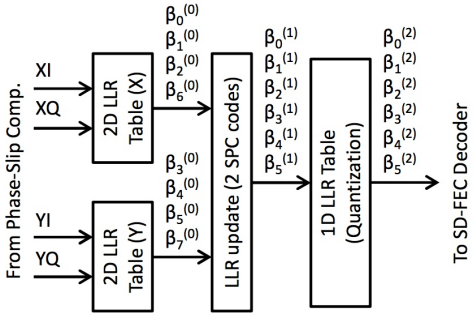

Fig. 12. Soft-demapping circuit for 6b4D-2A8PSK [44]

4.9. DSP Algorithm

1) Adaptive Equalizer:
So far, in order to analyze the fundamental potential of 4D-2A8PSK family, we used an idealized data-directed least-mean-square equalizer. In this section, we briefly address the performance impact with more realistic equalizers [50], [51] for practical implementation.
First, we consider a conventional radius-directed equalizer (RDE) [51] for 6b4D-2A8PSK, where the decision on the ring is carried out on each polarization independently. In this case, we observed a degradation of 0.12 dB and 0.10 dB in span loss budget compared to the idealized least-mean-square equalizer, respectively, at a launch power of -10 dBm and -4 dBm.
We then took advantage of 4D constant modulus property, by using the relative power of polarizations for soft decision of the ring radii. For soft-decision information, we used a sigmoid function $S(x) = 1/(1+e^{-x/a})$, where a is a parameter to determine the softness, and x is a relative power of two polarizations. In this manner, we could compensate for the degradation by 0.07 dB from the conventional RDE. Overall, the net degradation due to the realistic adaptive equalizer compared to the ideal one is no greater than 0.05 dB.

2) LLR Computation:
For SD-FEC, it is necessary to calculate log-likelihood ratio (LLR) with moderate circuit complexity. Recently, a new algorithm was proposed for fast-decoding and LLR-computation for high-order set partitioned 4D-QAM formats [52]. It was then extended to 6b4D-2A8PSK to use two lookup tables [44]. The schematic of the soft-demapping circuit is shown in Fig. 12. , and also used the asymmetry between the radial and the axial LLR and the offline processing of the experimental data showed only a small power penalty [44]. It also used the LLR calculation method robust against residual phase noise [53].

4.10. Experiment

We have also conducted a transmission experiment comparing 6b4D-2A8PSK and DP-Star-8QAM [44]. The signals were either 6b4D-2A8PSK or DP-Star-8QAM modulated at 32 GBaud and filtered with a root-riased cosine filtere with a roll-off factor of 0.15. 70 channels were spaced at 50

GHz spacing. The transmission line was 1,260 km, having an average span length of 70 km. Chromatic dispersion was managed in-line by the mixture of non-zero dispersion shifted fibre (NZDSF) having negative local CD of -3 ps/nm and standard single-mode fibre (SSMF). In the receiver side, the signal stored by 64 GS/s analogue-to-digital converters (ADCs) was processed offline, which included CD compensation, adaptive equalization with constant modulus algorithm for initial convergence and radius directed equalization afterward, carrier recovery (CR) with multi-pilot algorithm [50] having an window size of 63, pilot-aided phase-slip recovery, and the proposed soft-demapping as desribed in Sec. 4-9.
Figure 14 shows the experimental results; Fig. 14 (a) is Q from GMI as a function of launched power. In the case of ideal soft-demapping (only 16 level quantization for SD-FEC decoding was applied), we observed 0.6 dB improvement at maximum Q by 4D-2A8PSK compared to DP-Star-8QAM. The proposed technique had performance degradation of 0.15 dB and 0.06 dB for 4D-2A8PSK and DP-Star-8QAM, respectively, compared to the ideal LLR. The overall performance gain of 0.5 dB was still significant in the highly nonlinear transmissions. FIg. 14 (b) shows required OSNR, which was calculated by loading noise at the receiver DSP to emulate OSNR decrease. The target normalized GMI was set to 0.92, which was close to 20.5% SD-FEC limit [56]. The proposed soft-demmaping worked even at such low OSNR conditions and 4D-2A8PSK outperformed DP-Star-8QAM as the launched power increase.

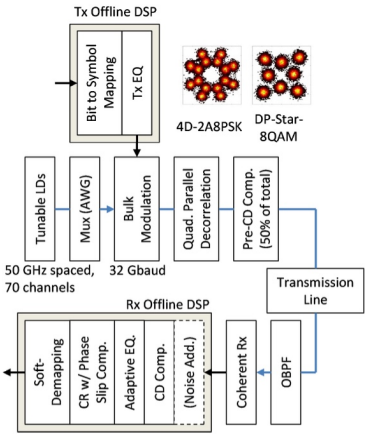

Fig. 13. Experimental setup [44].

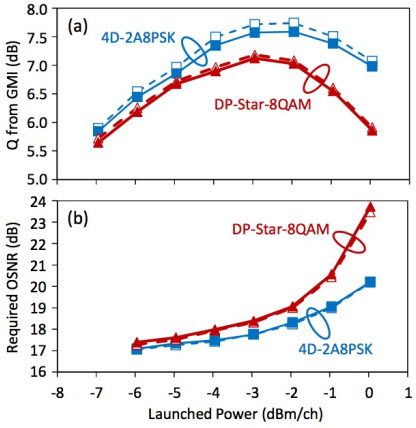

Fig. 14. Experimental result of (a) Q from GMI and (b) required OSNR for two types of LLR calculation: ideal (dotted line) and the proposed in Fig. 12 (solid line) [44].

4.11. Time Domain Hybrid Modulation

TDH modulation has been studied considerably to cover a wide range of channel conditions, due to its flexibility in choosing the nearly arbitrary spectral efficiency [12], [54], [55]. As the constituent modulation formats, we use DP-QPSK (4 bits/symbol) and QP-16QAM (8 bits/symbol) in conjunction with 5b4D, 6b4D, and 7b4D-2A8PSK to widen the range of TDH [57]. For a

comparison, we also use TDH modulation using conventional modulation formats, i.e., DP-QPSK, 32SP-QAM, DP-Star-8QAM (S8QAM), 128SP-QAM, and DP-16QAM. The benefit of the 4D-2A8PSK family is the 4D constant modulus property. In other words, there is no compromise in choosing the power ratio (ratio between the two modulation formats). On the other hand, conventional formats experience power fluctuations, causing compromise in the power ratio [29], [57].

We simulated transmission performance over the same link condition as described in Sec. 4.7. For 5b4D, 6b4D, and 7b4D-2A8PSK formats, we choose the ring ratio of 0.60, 0.65, and 0.59 for the best nonlinear performance. For all the THD modulation, we use 1:1 ratio with alternating formats, however, in actual systems, any arbitrary ratio can be used. The important parameter for TDH is the power ratio, i.e., how much power will be allocated for each time slot. We optimize the power ratio for the best nonlinear performance.

Fig. 15 shows the calculated span loss budget for 4-6 bits/symbol modulation formats, including the 2A8PSK-based and the conventional TDH modulation. DP-QPSK and 6b4D-2A8PSK data are also included as a reference. Fig. 16 shows the span loss budget for 6.5-8 bits/symbol modulation formats. From these figures, we can see that the TDH modulation based on 2A8PSK has much better nonlinear performance than that based on the conventional modulation formats, due to their constant modulus property.
The peak span loss budget for various spectral efficiency is shown in Fig. 17. Here, 4.5, 5.5, 6.5, 7.5 bits/symbol TDH based on 2A8PSK used DP-QPSK, 5b4D-2A8PSK, 6b4D-2A8PSK, 7b4D-2A8PSK, and DP-16QAM. TDH based on the conventional formats used DP-QPSK, 32SP-QAM, S8QAM, 128SP-QAM, and DP-16QAM. We observed 1.3, 1.6, 1.6, and 0.6 dB increase in peak span loss budget, when TDH used 2A8PSK, at 4.5, 5.5, 6.5, and 7.5 bits/symbol, respectivety. This shows the versatility of the 4D-2A8PSK family.

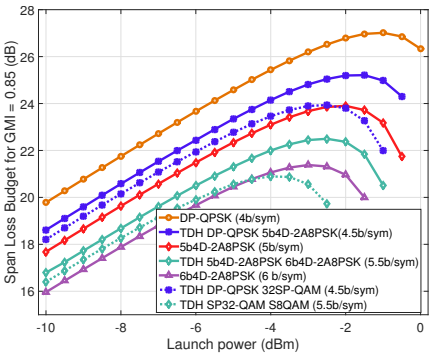

Fig. 15. Span loss budget for various modulation formats in the range of 4 - 6 bits/symbol [57].

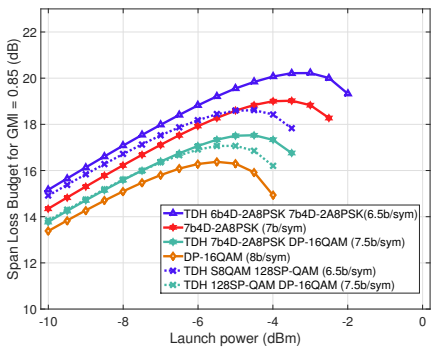

Fig. 16. Span loss budget for various modulation formats in the range of 6.5 - 8 bits/symbol [57].

4.12. 3.5 bits/symbol Modulation Format

Grassmann code [4], [58] to be robust against state of polarization (SOP) rotation including cross polarization modulation (XPolM) as described in Sec. 2. We investigated a Grassmann code-based 7-bit 8D code [59], whose schematic is shown in Fig. 18. 2-ary amplitude QPSK (2AQPSK)

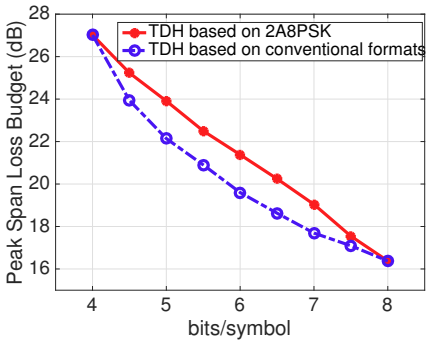

Fig. 17. Span loss budget for TDH modulation based on the 4D-2A8PSK formats, and that on the conventional modulation formats [57].

and 2A8PSK are used for the first and the second time slots, respectively. x_1, x_2, y_1, y_2 are x- and y-polarization component of the first and second time slot, respectively. Let b_0-b_6 the information bits. In a similar manner as described in Sec 4.7, for the 2AQPSK part, b_0 and b_1 are used for the angle of x_1, and b_2, b_2 are used for the angle of y_1, respectively. For x_2, b_4–b_6 are used for the angle representation of 2A8PSK. All use Gray coding for the angle. The radius of x_1 is expressed as $XOR(b_4,b_5,b_6)$, where ”0” means the larger radius, and "1" means the smaller radius. The ratio of the radii is called the ring ratio. The radius of y_1 is expressed as $\overline{XOR(b_4,b_5,b_6)}$. Both 2AQPSK and 2A8PSK share the same ring ratio of 0.70, which was optimized for the nonlinear performance. The radius of x_2 is expressed as $XOR(b_0,b_1,...,\ b_6)$. y_2 is calculated from the Grassmannian condition $x_1\ y_1^* + x_2\ y_2^* = 0$. This guarantees the 4D constant modulus condition for both time slots.

We compared 7b8D-2A8PSK (3.5bits/symbol), PS-QPSK (3bits/symbol), and DP-QPSK (4bits/symbol) of the same data rate. We also chose the channel spacing as 1.15 times of the Baud rate. Simulation procedures and parameters are nearly identical to that described in Sec. 4-71, except that we used 9 channels. The simulated results are shown in Fig. 19. 7b8D-Grassmann format exhibit almost the same span loss budget as PS-QPSK which has higher Baud rate and broader spectrum. On the other hand 7b8D-Grassmann format show much larger span loss than DP-QPSK, although the latter has narrower spectrum. Therefore, depending on the application, 7b8D-Grassmann format may be an alternative to PS-QPSK and DP-QPSK.

5. Conclusion

We reviewed the recently proposed 5, 6, and 7 bits/symbol 4D modulation format family based on 2A8PSK. A series of nonlinear transmission simulation results revealed that this modulation format family outperforms the conventional modulation formats at each corresponding spectral efficiency, in particular for highly nonlinear DM links. It was also confirmed that the primary benefit of the 4D constant modulus property comes from the reduction of SPM and XPM. Since these modulation formats differ just in the parity bits, they can be realized with very similar hardware over different spectral efficiency between DP-QPSK and DP-16QAM. Furthermore, these modulation format family can be a constituent of time domain hybrid modulation, where

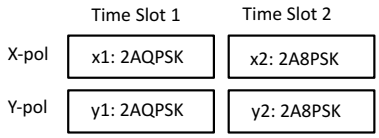

Fig. 18. Structure of the 7b8D-Grassmann code.

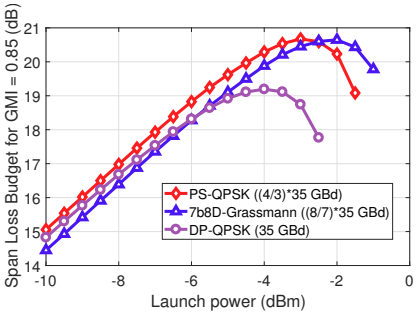

Fig. 19. Span loss budget of three modulation for the same data rate, as a function of launch power for the target normalized GMI = 0.85.

almost arbitrary spectral efficiency can be realized between 4 and 8 bits/symbol, combined with DP-QPAK and DP-16QAM.

References

[1] R.-J. Essiambre, G. Kramer, P. J. Winzer, G. J. Foschini, and B. Goebel, "Capacity Limits of Optical Fiber Networks," *J. Lightw. Technol.*, vo. 28, no. 4, pp. 662–701, 2010.

[2] M. Secondini, E. Forestieri, and G. Prati, "Achievable Information Rate in Nonlinear WDM Fiber-Optic Systems With Arbitrary Modulation Formats and Dispersion Maps,? *J. Lightw. Technol.*, vol. 31, no. 23, pp. 3839–3852, 2013.

[3] E. Agrell, A. Alvarado, G. Durisi, and M. Karlsson, "Capacity of a Nonlinear Optical Channel With Finite Memory,? *J. Lightw. Technol.*, vol. 32, no. 16, pp. 2862–2876, 2015.

[4] A. D. Shiner, M. Reimer, A. Borowiec, S. O. Gharan, J. Gaudette, P. Mehta, D. Charlton, K. Roberts, and M. O'Sullivan, "Demonstration of an 8-dimensional modulation format with reduced inter-channel nonlinearities in a polarization multiplexed coherent system," *Opt. Exp.*, vol. 22, no. 17, pp. 20366–20374, 2014.

[5] M. Jinno, B. Kozicki, H. Takara, A. Watanabe, Y. Sone, T. Tanaka, and A. Hirano, "Distance-adaptive spectrum resource allocation in spectrum-sliced elastic optical path network," *IEEE Commun. Mag.*, vol. 48, no. 8, pp. 138–145, 2010.

[6] A. Nag, M. Tornatore, and B. Mukherjee, "Optical network design with mixed line rates and multiple modulation formats," *J. Lightw. Technol.*, vol.28, no. 4, pp. 466–475, 2010.

[7] A. Alvarado, D. J. Ives, S. J. Savory, and P. Bayvel, "On the impact of optimal modulation and FEC overhead on future optical networks," *J. Lightw. Technol.*, vol. 34,, no. 9, pp. 2339–2352, 2016.

[8] D. J. Ives, A. Alvarado, and S. J. Savory, "Adaptive transceivers in nonlinear flexible networks," in *European Confrence on Optical Communication*, 2016, Düsseldorf, Germany, Paper M.1.B.1.

[9] E. Agrell and M. Karlsson, "Power-efficient modulation formats in coherent transmission systems," *J. Lightw. Technol.*, vol. 27, no. 22, pp. 5115–5126, 2009.

[10] G. Bosco, V. Curri, A. Carena, P. Poggiolini, and F. Forghieri, "On the performance of Nyquist-WDM terabit superchannels based on PM-BPSK, PM-QPSK, PM-8QAM or PM-16QAM subcarriers," *J. Lightw. Technol.*, vo. 29, no. 1, pp. 53–61, 2011.

[11] J. Renaudier, A. Voicila, O. Bertran-Pardo, O. Rival, M. Karlsson, G. Charlet, and S. Bigo, "Comparison of set-partitioned two-polarization 16QAM formats with PDM-QPSK and PDM-8QAM for optical transmission systems with error-correction coding," in *European Conf. Optical Communications*, 2012, Amsterdam, The Netherlands, Paper We.1.C.5.

[12] Q. Zhuge, X. Xu, M. Morsy-Osman, M. Chagnon, M. Qiu, and D. V. Plant, "Time domain hybrid QAM based rate-adaptive optical transmissions using high speed DACs," in *Optical Fiber Commun. Conf.*, 2013, Anaheim, CA, Paper OTh4E.6.

[13] J. K. Fischer, S. Alreesh, R. Elschner, F. Frey, M. Nölle, C. Schubert, "Bandwidth-variable transceivers based on 4D modulation formats for future flexible networks," in *European Conf. Optical Communications*, 2013, London, UK, Paper Tu.3.C.1.

[14] D. S. Millar, T. Koike-Akino, S. Ö. Arik, K. Kojima, T. Yoshida, and K. Parsons, "High-dimensional modulation for coherent optical communications systems," *Opt. Exp.*, vol. 22, no. 7, pp. 8798–8812, 2014.

[15] M. Reimer, S. O. Gharan, A. D. Shiner, and M. O'Sullivan, "Optimized 4 and 8 dimensional modulation formats for variable capacity in optical networks," in *Optical Fiber Commun. Conf.*, 2016, Anaheim, CA, Paper M3A.4

[16] T. Koike-Akino, K. Kojima, D. S. Millar, K. Parsons, T. Yoshida, and T. Sugihara, "Pareto-efficient set of modulation and coding based on RGMI in nonlinear fiber transmissions," in *Optical Fiber Commun. Conf.*, 2016, Anaheim, CA, Paper Th1D.4.

[17] T. Koike-Akino, K. Kojima, D. S. Millar, K. Parsons, T. Yoshida, and T. Sugihara, "Pareto optimization of adaptive modulation and coding set in nonlinear fiber-optic systems," *J. Lightw. Technol.*, vol. 35, no. 3, pp.1-9, 2017.

[18] X. Liu, A. R. Chraplyvy, P. J. Winzer, R. W. Tkach, and S. Chandrasekhar, "Phase-conjugated twin waves for communication beyond the Kerr nonlinearity limit,? *Natue Photonics*, vol. 7, pp. 560–568, 2013.

[19] M. Chagnon, M. Osman, Q. Zhuge, X. Xu, and D. V. Plant, "Analysis and experimental demonstration of novel 8PolSK-QPSK modulatoin at 5 bis/symbol for passive mitigation of nonlinear impairments," *Opt. Exp.*, vol. 21, no. 25, pp. 30204–30220, 2013.

[20] H. Bülow, "Polarization QAM Modulation (POL-QAM) for Coherent Detection Schemes," in *Optical Fiber Commun. Conf.*, 2009, San Diego, CA, Paper OWG2.

[21] M. Sjödin, E. Agrell, and M. Karlsson, "Subset-optimized polarization-multiplexed PSK for fiber-optic communications," *IEEE Comm. Lett.*, vol. 17, no. 5, pp. 838–840, 2013.

[22] H. Buelow, X. Lu, L. Schmalen, A. Klekamp, and F. Buchali, "Experimental performance of 4D optimized constellation alternatives for PM-8QAM and PM-16QAM," in *Optical Fiber Commun. Conf.*, 2014, San Francisco, CA, Paper M2A.6.

[23] R. Rios-Mueller, J. Renaudier, L. Schmalen, and G. Charlet, "Joint coding rate and modulation format optimization for 8QAM constellations using BICM mutual information," in *Optical Fiber Commun. Conf.*, 2015, Los Angeles, CA, Paper W3K.4.

[24] S. Zhang, K. Nakamura, F. Yaman, E. Mateo, T. Inoue, Y. Inada, "Optimized BICM-8QAM formats based on generalized mutual information," in *European Conf. Optical Communications*, 2015, Valencia, Spain, Paper Mo.3.6.5.

[25] T. Nakamura, E. L. T. d. Gabory, H. Noguchi, W. Maeda, J. Abe, and K. Fukuchi, "Long haul transmission of four-dimensional 64SP-12QAM signal based on 16QAM constellation for longer distance at same spectral efficiency as PM-8QAM," in *European Conf. Optical Communications*, 2015, Valencia, Spain, Paper Th.2.2.2.

[26] K. Kojima, D. S. Millar, T. Koike-Akino, and K. Parsons, "Constant modulus 4D optimized constellation alternative for DP-8QAM," in *European Conf. Optical Communications*, 2014, Cannes, France, Paper P.3.25.

[27] K. Kojima, T. Koike-Akino, D. S. Millar, and K. Parsons, "BICM capacity analysis of 8QAM-alternative modulation formats in nonlinear fiber transmission," *Tyrrhenian Int'l Workshop on Digital Comm.*, 2015, Florence, Italy, Paper P.4.5.

[28] K. Kojima, T. Koike-Akino, D. S. Millar, T. Yoshida, and K. Parsons, "BICM capacity analysis of 8QAM-alternative 2D/4D modulation formats in nonlinear fiber transmission," in *Conf. Lasers and Electro-Optics*, 2016, Anaheim, Paper SM2F.5.

[29] K. Kojima, T. Yoshida, T. Koike-Akino, D. S. Millar, K. Parsons, and V. Arlunno, "5 and 7 bit/symbol 4D Modulation Formats Based on 2A8PSK," in *European Conf. Optical Communications*, 2016, Düsseldorf, Germany, Paper W.2.D.1.

[30] K. Kojima, T. Yoshida, T. Koike-Akino, D. S. Millar, K. Parsons, M. Pajovic, and V. Arlunno, "Nonlinearity-tolerant four-dimensional 2A8PSK family for 5-7 bits/symbol spectral efficiency," *J. Lightw. Technol.*, vol. 33, no. 10, pp. 1993–2003, 2015.

[31] D. S.‘Millar, T.‘Koike-Akino, K.‘Kojima, and K. Parsons, “A 24-Dimensional Modulation Format Achieving 6 dB Asymptotic Power Efficiency,? in *Signal Processing in Photonic Communications*, 2013, Puerto Rico, Paper SPM3D.6.

[32] T. A. Eriksson, P. Johannisson, M. Sjödin, E. Agrell, P. A. Andrekson, and M. Karlsson, “Frequency and polarization switched QPSK," *European Conf. Optical Communications*, 2013, London, UK, Paper Th.2.D.4.

[33] T. Koike-Akino, D. S. Millar, K. Kojima, and K Parsons, “Eight-Dimensional Modulation for Coherent Optical Communications,? *European Conf. Optical Communications*, 2013, London, UK, Paper Tu.3.C.3.

[34] D. S. Millar, T. Koike-Akino, R. Maher, D. Lavery, M. Paskov, K. Kojima, K. Parsons, B. C. Thomsen, S. J. Savory, P. Bayvel, “Experimental demonstration of 24-dimensional extended Golay coded modulation with LDPC,” in *Optical Fiber Commun. Conf.*, 2014, San Francisco, CA, Paper M2I.2.

[35] D. S. Millar, T. Koike-Akino, S. Ö. Arik, K. Kojima, and K. Parsons, “Comparison of quaternary block-coding and sphere-cutting for high-dimensional modulation,” in *Optical Fiber Commun. Conf.*, 2014, San Francisco, CA, Paper M3A.4.

[36] A. Alvarado, E. Agrell, D. Lavery, and P. Bayvel, “LDPC codes for optical channels: Is the “FEC Limit” a good predictor of post-FEC BER?” in *Optical Fiber Commun. Conf.*, 2015, Los Angeles, CA, Paper Th3E.5.

[37] A. Alvarado and E. Agrell, “Four-dimensional coded modulation with bit-wise decoders for future optical communications,” *J. Lightw. Technol.*, vol. 35, no. 8, pp. 1383–1391, 2017.

[38] R. Maher, A. Alvarado, D. Lavery, and E. P. Bayvel, “Modulation order and code rate optimisation for digital coherent transceivers using generalised mutual information,” in *European Conf. Optical Communications*, 2015, Valencia, Spain, Paper M.3.3.4.

[39] S. ten Brink, G. Kramer, and A. Ashikhmin, “Design of low-density parity-check codes for modulation and detection,” *IEEE Trans. Commun.*, vol. 52, no. 4, pp. 670–678, Apr. 2004.

[40] A. Bennatan and D. Bushtein, “Design and analysis of nonbinary LDPC codes for arbitrary discrete-memoryless channels,” *IEEE Trans. Inf. Theory*, vol. 52, no. 2, pp. 549–583, 2006.

[41] L. Szczecinski and A. Alvarado, *Bit-interleaved coded modulation: Fundamentals, analysis, and design*, Wiley, UK, 2015, p. 228.

[42] S. Zhang, M. Arabaci, F. Yaman, I. B. Djordjevic, L. Xu, T. Wnag, Y. Inada, T. Ogata, and Y. Aoki, “Experimental study of non-binary LDPC coding for long-haul coherent optical QPSK transmissions,” *Opt. Exp.*, vol. 19, no. 20, pp. 19042–19049, 2011.

[43] K. Sugihara, Y. Miyata, T. Sugihara, K. Kubo, H. Yoshida, W. Matsumoto, and T. Mizuochi, “A spatially-coupled type LDPC code with an NCG of 12 dB for optical transmission beyond 100 Gb/s,” in *Optical Fiber Commun. Conf.*, 2013, Anaheim, CA, Paper OM2B.4.

[44] T. Yoshida, K. Matsuda, K. Kojima, H. Miura, D. Dohi, M. Pajovic, T. Koike-Akino, D. S. Millar, K. Parsons, and T. Sugihara, “Hardware-efficient precise and flexible soft-demapping for multi-dimensional complementary APSK signals,” in *European Conf. Optical Communications*, 2016, Düsseldorf, Germany, Paper Th.2.P2.SC3.27.

[45] K. Kojima, T. Koike-Akino, D. S. Millar, M. Pajovic, K. Parsons, and T. Yoshida,, “Investigation of low code rate DP-8PSK as an alternative to DP-QPSK,” in *Optical Fiber Commun. Conf.*, 2016, Anaheim, CA, Paper Th1D.2.

[46] P. Poggiolini, G. Bosco, A. Carena, V. Curri, and F. Forghieri, “Performance evaluation of coherent WDM PS-QPSK (HEXA) accounting for non-linear fiber propagation effects,” *Opt. Exp.*, vol. 18, no. 11, pp. 11360–11371, 2010.

[47] N. Rossi, P. Serena, and A. Bononi, “Symbol-rate dependence of dominant nonlinearityand reach in coherent WDM links,” *J. Lightw. Technol.*, vol. 33, no. 14, pp. 3132–3143, 2009.

[48] A. Bononi, P. Serena, N. Rossi, and D. Sperti, “Which is the dominant nonlinearity in long-haul PDM-QPSK coherent transmissions?,” in *European Conf. Optical Communications*, 2010, Torino, Italy, Paper Th.10.E.1.

[49] M. Winter, C.-A. Burge, D. Setti, and K. Petermann, “A statistical treatment of cross-polarization modulation in DWDM systems,” *J. Lightw. Technol.*, vol. 27, no. 17, pp. 3739–3751, 2009.

[50] M. Pajovic, D. S. Millar, T. Koike-Akino, R. Maher, D. Lavery, A. Alvarado, M. Paskov, K. Kojima, K. Parsons, B. C. Thomsen, S. J. Savory, and P. Bayvel, “Experimental demonstration of multi-pilot aided carrier phase estimation for DP-16QAM and DP-256QAM,” in *European Conf. Optical Communications*, 2015, Valencia, Spain, Paper Mo.4.3.3.

[51] M. J. Ready and R. P. Gooch, “Blind equalization based on radius directed adaptation,” *Proc. of ICASSP*, vol. 3, pp. 1699–1702, 1990.

[52] S. Ishimura and K. Kikuchi, “Fast decoding and LLR-computation algorithms for high-order set-partitioned 4D-QAM constellations.” in *European Conf. Optical Communications*, 2015, Valencia, Paper P.3.01.

[53] T. Koike-Akino, D. S. Millar, K. Kojima, and K. Parsons, “Phase noise-robust LLR calculation with linear/bilinear transform for LDPC-coded coherent communications," *Conf. Lasers and Electro-Optics*, 2015, San Diego, Paper SW1M.3.

[54] X. Zhou, L. E. Nelson, R. Isaac, P. D. Magill, B. Zhu, P. Borel, K. Carlson, and D. W. Peckham, “12,000km transmission of 100GHz spaced, 8x495-Gb/s PDM time-domain hybrid QPSK-8QAM signals, " in *Optical Fiber Commun. Conf.*, 2012, Los Angeles, CA, Paper OTu2B.4.

[55] L. Yan et al., “Sensitivity comparison of time domain hybrid modulation and rate adaptive coding," Proc. OFC, W1I.3, Anaheim (2013).

[56] K. Ishii, K. Dohi, K. Kubo, K. Sugihara, Y. Miyata, and T. Sugihara, “A study on power-scaling of triple-concatenated FEC for optical transport networks," in *European Conf. Optical Communications*, 2015, Valencia, Paper Tu3.4.2.

[57] K. Kojima, T. Yoshida, K. Parsons, T. Koike-Akino, D. S. Millar, and K. Matsuda, “Nonlinearity-tolerant time domain hybrid modulation for 4-8 bits/symbol based on 2A8PSK," in *Optical Fiber Commun. Conf.*, 2017, Los Angeles, CA, Paper W4A.5.

[58] T. Koike-Akino, K. Kojima, and K. Parsons, “Trellis-coded high-dimensional modulation for polarization crosstalk self cancellation in coherent optical communications," in *Signal Processing in Photonic Communications*, 2015, Boston, Paper SpS3D.6.

[59] K. Kojima, T. Yoshida, T. Koike-Akino, D. S. Millar, K. Matsuda and K. Parsons, “Nonlinearity-tolerant modulation formats at 3.5 bits/symbol," *Conf. Lasers and Electro-Optics*, 2017, San Jose, Paper STu4M.3.